Prediction of Water Inflow at Tunnel-Fault Intersection—A Case Study of a Tunnel in Shantou

Wei Hao, Jian Zhang, Yan Xu*

College of Construction Engineering, Jilin University, Changchun, Jilin 130012, China
China Railway Design corporation, Tianjin 300251, China
*Correspondence Author, 471348028@qq.com

Abstract: *Water inflow is a common geological hazard in tunnel engineering. Particularly the tunnel sections located within fault zones are prone to severe water inflow. Taking the tunnel faults in Shantou City as a case, this study analyzes the topography, lithology, geological structure, and hydrogeological conditions of F1 and F7 faults. Based on the faults conditions, groundwater dynamics method was selected to calculate the water inflow into tunnel. The unit water inflow was used to classify water abundance at tunnel faults. The results show that the unit water inflow of F1 and F7 faults in tunnel exceeds 10.0 m²/d, indicating a strong rich in water. It is recommended to enhance preventive and drainage measures and improve advance geological forecasting.*

Keywords: Fault, Water inflow, Water abundance degree, Groundwater dynamics method.

1. Introduction

Water inflow has long been a significant issue in tunnel engineering. It will pose serious safety risks and results in substantial economic losses (Zhen et al. 2014). This risk is particularly heightened when tunneling through fractured fault zones with high groundwater levels (Ruan et al. 2022). Therefore, it is essential to assess the hydrogeological conditions of these fractured fault zones, accurately predict water inflow and provide reliable geological parameters for design (Chen et al. 2021).

The main methods for predicting water inflow in tunnels include the atmospheric rainfall infiltration method, underground runoff modulus method, groundwater dynamics method, and engineering analogy method (Xu et al. 2017). Numerous research have investigated water inflow hazards at tunnel faults. Chen et al. (2024) conducted a study on a proposed mountain tunnel, utilizing various methods, including the atmospheric rainfall infiltration method and groundwater dynamics method, to predict water inflow. The results derived from these methods were analyzed to confirm the maximum water inflow and normal water inflow. Zhang et al. (2023) used the atmospheric rainfall infiltration method and underground runoff modulus method to predict the water inflow of a water-rich tunnel in Chongqing. Additionally, the case incorporated long-term in-situ hydrogeological observations to develop a predictive method for water inflow in the tunnel. Wang et al. (2021) employed statistical methods and Gray Relational Analysis (GRA) to examine the relationship between fault complexity and water inflow in mines, exploring how fault development influences water inflow in mining operations.

Numerous research have demonstrated a strong correlation between water inflow and faults. The rock mass surrounding faults is typically highly fractured, with these shattered zones acting as reservoirs for groundwater (Wu et al. 2020). Taking the tunnel faults in Shantou City as a case, this study assesses the possibility of water inflow by analyzing the lithology, geological structures, and hydrogeological conditions at tunnel faults. Appropriate calculation formulas for groundwater recharge in mountainous areas with fault conditions were utilized to predict the amount of water inflow and analyze the water abundance at tunnel faults.

2. Project Overview

The tunnel extends across Haojiang and Longhu districts in Shantou City, near the China South Sea. The terrain is characterized by slightly surface relief, with a natural slope gradient ranging from 20° to 30°. The landform is erosion hilly topography. The tunnel has a maximum burial depth of approximately 180 meters, which was primarily constructed by mining methods.

3. Analysis of Geological Conditions

3.1 Stratum Lithology

The primary strata of this tunnel include the Holocene Quaternary strata (Q_4), the third intrusive granite (γ_y^3) of Yanshan period, and the fifth intrusive granite (γ_y^5) of Yanshan period. The stratigraphic profiles of F1 and F7 faults are shown in Figure 1 and Figure 2.
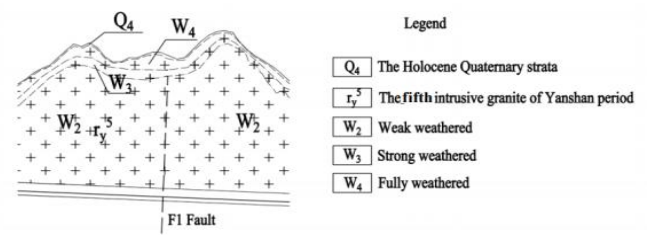
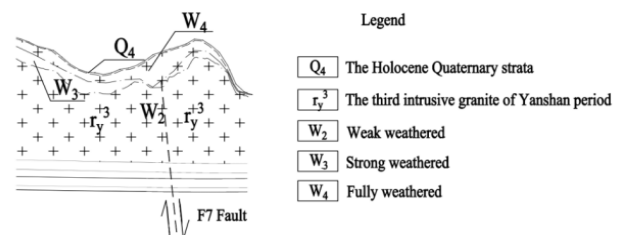

Figure 1: Stratigraphic profile of the F1 fault

Figure 2: Stratigraphic profile of the F7 fault

3.2 Geological Structure

Based on regional geological data, field surveys along the tunnel route, and seismic exploration, along with high-frequency magnetotelluric sounding (EH-4) and high-density resistivity methods, the tunnel intersects several faults, among which the F1 and F7 faults are large in scale. The water inflow is mainly studied for these two faults.

F1 fault is a large regional fault, which cuts the fifth intrusive granite (γ_y^5) of Yanshan period. The shattered fault zone is characterized by developed joints and fragmented rock mass. In-situ drilling reveals diabase dykes near F1 fault, with well-developed joints and fragmented rock masses. The rock cores are predominantly blocky and short columnar shapes, with fragments shapes in certain sections. Based on laboratory permeability test data and experience from Shantou area, the permeability coefficient of rock mass in shattered fault zone is 0.221m/d, classifying its permeability as medium.

F7 fault is a large regional fault, which cuts the third intrusive granite (γ_y^3) of Yanshan period. The shattered fault zone is characterized by developed joints and fragmented rock mass. Based on laboratory permeability test data and experience from Shantou area, the permeability coefficient of rock mass in shattered fault zone is 0.221m/d, classifying its permeability as medium.

3.3 Hydrogeological Condition

Groundwater in the F1 and F7 faults primarily consists of fissure water. The water-bearing stratum of massive rock fissure water is primarily granite of Yanshan period. Groundwater is stored in rock fissures, which are mainly weathered fractures with thick weathering zones. Structural fissure water is stored in structural fracture zones, primarily located near two shattered fault zones. Fissure water in the massive rocks is mainly replenished by atmospheric precipitation and runoff from gullies. Bedrock fissure water is primarily discharged as springs along weathered fractures and structural fissures in gullies or deep cuts. Some bedrock fissure water also recharges as subsurface flow to deep fissures or provides lateral recharge to the loose rocks pore water in plain areas.

4. Water Inflow Prediction

An analysis of the engineering geological conditions at two faults reveals that the water-bearing stratum of massive rock fissures is primarily granite of Yanshan period. The structural fissure water is located within the structural fracture zone. The thickness of tunnel's water-bearing stratum is limited. The weakly weathered granite in tunnel has very low permeability, acting as an impermeable basement that is horizontally oriented. Groundwater flow is laminar, with water entering the tunnel from one side. These conditions align with the requirements for applying the calculation formula for groundwater recharge in mountainous regions. Therefore, the calculation formula for groundwater recharge in mountainous regions was selected to predict water inflow at tunnel faults.

4.1 Groundwater Dynamics Method

The calculation formula for groundwater recharge in mountainous regions is presented in Eq. (1).

$$Q = BK \left[\frac{(H_1^2 - h^2)}{2R} + H_0 q_r \right] \qquad (1)$$

where Q is the tunnel water inflow (m³/d); B is the length of tunnel through water-bearing stratum (m); K is the permeability coefficient of water-bearing stratum (m/d); r is half width of the tunnel (m); R is the influence radius of tunnel water inflow (m); H_1 is the depth of static water level to tunnel bottom (m); h is the height of drawdown curve on tunnel side wall (m), in this case $h=0$; H_0 is the depth of water level drawdown (m), $H_0 = H_1 - h$; qr is the reduced seepage rate, $q_r = f(\alpha, \beta); \alpha = \frac{R}{R+r}, \beta = \frac{R}{T}$, qr is obtained from Figure 3 after calculating α and β values.
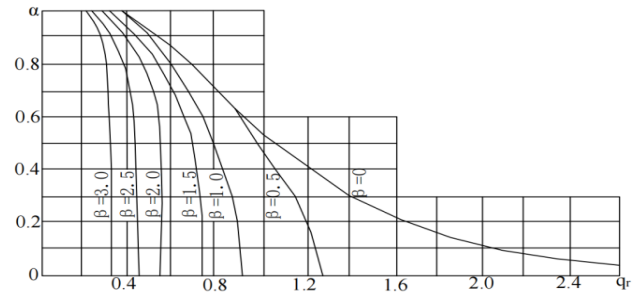

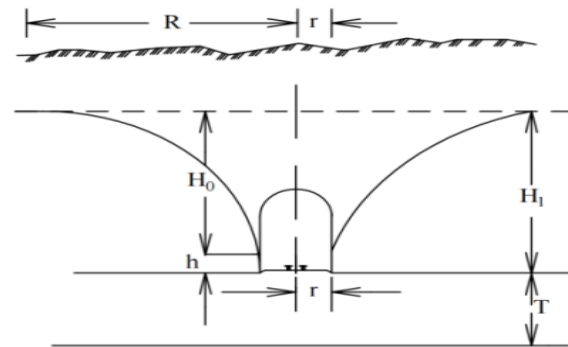**Figure 3:** Relation graph of $q_r = f(\alpha, \beta)$

Figure 4: Tunnel inflow calculation diagram

Field pumping test was carried out to obtain the permeability coefficient of water-bearing stratum K, the influence radius of tunnel water inflow R, the depth of water level drawdown H_0 and the depth of static water level to tunnel bottom H_1. Geophysical exploration data was used to obtain the length of tunnel through water-bearing stratum B. The water inflow predicted at tunnel faults is shown in Table 1.

Table 1: Calculation table of tunnel groundwater dynamics method

Fault	The length of tunnel through water-bearing stratum B (m)	The permeability coefficient of water-bearing stratum K (m/d)	The depth of static water level to tunnel bottom H_1(m)	The depth of water level drawdown H_0(m)	The influence radius of tunnel water inflow R(m)	The width of the tunnel b(m)	The reduced seepage rate qr	The unit water inflow qs (m²/d)	The tunnel water inflow Q (m³/d)
F1	95	0.221	127.65	127.65	135.6	14	0.192	18.7	1776.5
F7	90	0.221	108.32	108.32	106.0	14	0.187	16.7	1503

4.2 Water Abundance

In tunnel construction, the degree of groundwater abundance in water-bearing stratum is categorized into different zones based on the unit water inflow. The specific zones are shown in Table 2.

Table 2: Zoning of water-bearing stratum abundance

item zoning	Water-shortage area	Weak watery area	Medium watery area	Strong rich in water
The unit water inflow qs(m²/d)	$qs<1$	$1 \leq qs<5$	$5 \leq qs<10$	$qs \geq 10$

The unit water inflow of F1 and F7 faults exceeds 10.0 m²/d, indicating a strong rich in water. Surface water is very likely to infiltrate the tunnel through shattered fault zones, which is speculated to have a significant impact on the tunnel construction. Joints are developed in tunnel fault belts. The rock mass is less-fragmentized. The faulted section serves as an effective water conduction channel. Therefore, it is recommended to enhance preventive and drainage measures and improve advance geological forecasting before construction and excavation.

5. Conclusion

(1) Based on regional geological data, field surveys along the tunnel route, and seismic exploration, along with high-frequency magnetotelluric sounding (EH-4) and high-density resistivity methods, the tunnel intersects several faults, among which F1 and F7 faults are large in scale. The permeability coefficient of rock mass in two faults is 0.221 m/d, classifying its permeability as medium. Joints are developed in the shattered fault zone. The rock mass is fragmented, which will lead to water inflow.

(2) The groundwater dynamics method and groundwater recharge calculation formulas in mountainous regions was applied to calculate the unit water inflow. The unit water inflow at F1 and F7 faults are 18.7 m²/d and 16.7 m²/d, all of which exceeds 10.0 m²/d, indicating a strong rich in water. It is recommended to enhance preventive and drainage measures and improve advance geological forecasting.

References

[1] ZHEN W, ZUO CQ, WU PP, et al. Study on the cause analysis and prediction of water inflow in Daping mountain tunnel[J]. Sino-foreign highway, 2014, 34(06): 184-188.

[2] RUAN ZG, LIU N. Prediction of water inflow in fault fracture zone of double-hole tunnel [J]. Journal of Railway Science and Engineering, 2022, 19(07): 1977-1984.

[3] CHEN J, ZHAO H, ZHAN JX. Analysis of hydrogeological conditions and prediction of water inflow in F1 fault zone tunnel of Hejiang branch tunnel[C]//Chinese hydraulic engineering society. The second volume of the papers of the 2021 academic annual meeting of Chinese Hydraulic Engineering Society, 2021:6.

[4] XU GX, Y J. Practice and Construction of Groundwater Treatment in Long Tunnel Construction[J]. Water Technical, 2017, 48(08):101-106.

[5] Chen Y, Liu M, Su M, et al. Prediction of water inflow and analysis of surrounding rock stability in unfavorable geological mountain tunnel[J]. Frontiers in Earth Science, 2024, 12.

[6] Zhang X, Wang M, Feng D, et al. Water Inflow Amount Prediction for Karst Tunnel with Steady Seepage Conditions [J]. Sustainability, 2023, 15(13).

[7] Wang, Dandan, Sui, et al. Hydrogeological Effects of Fault Geometry for Analysing Groundwater Inflow in a Coal Mine [J]. Mine Water and the Environment, 2021, 41(1):1-10.

[8] Wu J, J W, L W, et al. Prediction of water inflow into a tunnel based on three-district zoning of faults[J].IOP Conference Series: Earth and Environmental Science, 2020, 570(2):022070-.

[9] MA XH. Analyze the formation mechanism and comprehensive treatment policy of large water gushing (inrush) zone in Maoba No.1 tunnel based on the analysis of geological and hydrogeological basis[J]. Sichuan Building Materials, 2010, 36(04):139-141.

[10] Li S, He P, Li L, et al. Gaussian process model of water inflow prediction in tunnelconstruction and its engineering applications [J]. Tunnelling and Underground Space Technology incorporating Trenchless Technology Research, 2017, 69155-161.

[11] Jing W, Li W, Ni Y L, et al. Prediction of Water Inflow into Tunnel Crossing Intersecting Faults Based on IDB Seepage Model[J]. Geotechnical and Geological Engineering, 2022, 40(8):4041-4056.

[12] Li G, Li C, Liao J, et al. A New Hydro-Mechanical Coupling Numerical Model for Predicting Water Inflow in Karst Tunnels Considering Deformable Fracture [J]. Sustainability, 2023, 15(20).

[13] Lihu D, He W, Danqing S, et al. Analysis of the Catastrophe Mechanism and Treatment Countermeasures of a Sudden Water Inrush Disaster in a Long and Deeply Buried Tunnelin the Karst Area [J]. Journal of Performance of Constructed Facilities, 2023, 37(6).

[14] Samadi H, Mahmoodzadeh A, Elhag B A, et al. Application of hybrid-optimized and stacking-ensemble labeled neural networks to predict water inflow in drill-and-blast tunnels [J]. Tunnelling and Underground Space Technology incorporating Trenchless Technology Research, 2025, 156 106273-106273.

[15] Ding Y, Yin S, Dai Z, et al. Multi-Factor Prediction of Water Inflow from the Working Face Based on an Improved SSA-RG-MHA Model [J]. Water, 2024, 16 (23): 3390-3390.

[16] Chen K, Ren S, Li Z, et al. Investigation on the seepage-stress field evolution mechanism and failure process of karst tunnels in water-rich areas [J]. Environmental Earth Sciences, 2024, 83 (22): 638-638.